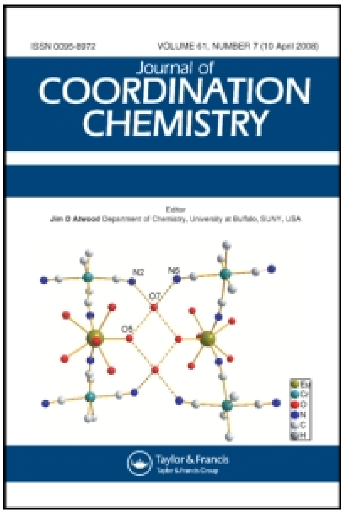

Journal of Coordination Chemistry
Publication details, including instructions for authors and subscription information:
http://www.informaworld.com/smpp/title~content=t713455674

Photochemical and electrochemical properties of porphyrin dimers containing an anhydride spacer

Huanbao Fa[a]; Wei Yin[a]; Changjun Hou[a]; Wenqi Zheng[b]; Dejun Wang[c]; Xingqiao Wang[c]
[a] College of Chemistry and Chemical Engineering, Chongqing University, Chongqing 400044, PR China [b] Jilin Architectural and Civil Engineering Institute, Changchun 130021, PR China [c] College of Chemistry, Jilin University, Changchun 130021, PR China

To cite this Article Fa, Huanbao , Yin, Wei , Hou, Changjun , Zheng, Wenqi , Wang, Dejun and Wang, Xingqiao(2009) 'Photochemical and electrochemical properties of porphyrin dimers containing an anhydride spacer', Journal of Coordination Chemistry, 62: 7, 1151 — 1161, First published on: 29 July 2010 (iFirst)

To link to this Article: DOI: 10.1080/00958970802382875

URL: http://dx.doi.org/10.1080/00958970802382875

Journal of Coordination Chemistry
Vol. 62, No. 7, 10 April 2009, 1151–1161

Taylor & Francis
Taylor & Francis Group

Photochemical and electrochemical properties of porphyrin dimers containing an anhydride spacer

HUANBAO FA†, WEI YIN†, CHANGJUN HOU†, WENQI ZHENG‡, DEJUN WANG§ and XINGQIAO WANG*§

†College of Chemistry and Chemical Engineering, Chongqing University, Chongqing 400044, PR China
‡Jilin Architectural and Civil Engineering Institute, Changchun 130021, PR China
§College of Chemistry, Jilin University, Changchun 130021, PR China

(*Received 20 February 2008; in final form 16 June 2008*)

A study on thermogravimetric analyses, surface photovoltage (SPV), electron paramagnetic resonance and electrochemical properties comparing a porphyrin dimer with that of corresponding monomer was presented. The SPV intensity is weaker than that corresponding monomer, and with field-induced surface photovoltage spectroscopy (FISPS) reveal that all the compounds are *p*-type semiconductors. The spectral bands of all the porphyrins corresponded to $\pi \rightarrow \pi^*$ transitions. Electrons (or holes) can be trapped on the porphyrins by applying both light and negative (or positive) electric field. The electrochemistry and EPR of the porphyrins show clearly that a π–π interaction existed between the two macrocycles of the dimer.

Keywords: Porphyrin dimer; Electrochemical and photochemical properties; Surface photovoltage spectroscopy

1. Introduction

Multiporphyrins display rich photophysical and electrochemical properties making them ideal for energy and electron transfers [1], molecular binding [2], multielectron redox catalysis [3], light harvesting [4] and organic magnetic materials [5]. The control of electronic interactions in bridged multiporphyrins was a crucial factor for the rational design of photonic molecular devices, particularly important for development of devices featuring a cascade of electron- or energy-transfer steps to achieve efficient excited-state energy transport or long-lived charge-separated states [6, 7]. Electronic communication was also important for design of optoelectronic devices [8, 9] and mixed-valence compounds [10]. Distance, geometry, and orientation have been recognized as important factors for control of communication with individual molecules within bridged multicomponents. In covalently linked multiporphyrin arrays that exhibit light-harvesting properties, the linker served both a mechanical function and an electronic function. The mechanical function was to hold the

---

*Corresponding author. Email: wangxingqiao@mail.jlu.edu.cn

Journal of Coordination Chemistry
ISSN 0095-8972 print/ISSN 1029-0389 online © 2009 Taylor & Francis
DOI: 10.1080/00958970802382875

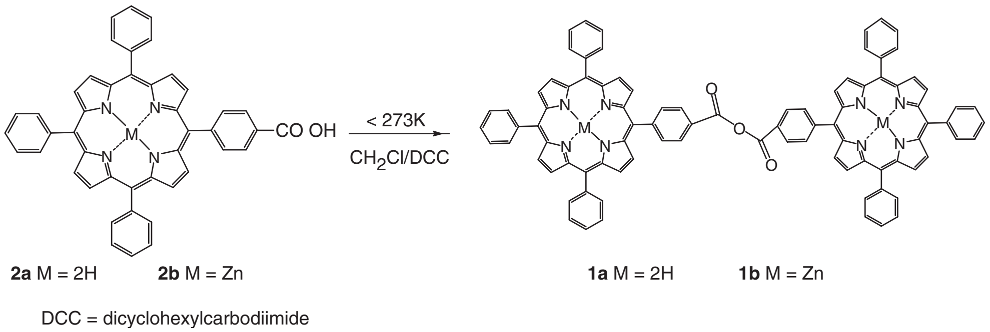

Scheme 1. Synthesis of diporphyrin derivatives.

porphyrins in a fixed architecture. The electronic function was to provide a conduit for communication among the porphyrins, thereby enhancing the rate and yield of excited-state energy transfer. Porphyrin chromophores have been assembled in many ways, connected directly with covalent bonds [11] and spacers such as other π-systems [12], hydrocarbon chains [13], transition metal complexes [14] and hydrogen-bonding molecules [15]. The porphyrin dimer containing anhydride linkage in a one-step, one-pot synthesis starting from porphyirn monomer had been synthesized [16a] (scheme 1). We also made a preliminary study on fluorescence properties comparing with that of corresponding monomer [16b].

In order to further understand electronic interactions in bridged metal-free and zinc porphyrin dimers, in this paper we present a preliminary study on their thermogravimetric analyses, surface photovoltage, electron paramagnetic resonance (EPR) and electrochemical properties comparing with the corresponding monomers.

2. Experimental

2.1. *Instrumentation and methods*

TGA analyses were carried out in a TGA instrument (TA Instruments SDT 2960 ± Simultaneous DTA-TGA ± Thermal Analyst 2100), in dry air with a heating rate of $10^\circ C\,min^{-1}$, from 30 to 800°C. The surface photovoltage spectroscopy (SPS) instrument was made by us. Monochromatic light was obtained by passing light of a 500W xenon lamp (CHF XQ500W, Global xenon lamp power) through a double-prism monochromator (Hilger and Watts, D 300). The slit width of entrance and exit is 1 mm. A lock-in amplifier (SR830-DSP), synchronized with a light chopper (SR540), was employed to amplify the photovoltage signal. The range of modulating frequency was from 20 to 70 Hz. The spectral resolution was 1 nm. The raw SPS data were normalized using the illuminometer (Zolix UOM-1S). Surface photovoltage spectroscopy was measured with a solid junction photovoltaic cell (ITO/sample/ITO) using a light source-monochromator-lock-in detection technique. The electron paramagnetic resonance (EPR) spectra were recorded on a JES-FE3AX ESR spectrometer. All measurements were carried out using solid samples at 100 kHz: 9.44 GHz microwave power and time constant: 0.03 s. Cyclic voltammetry was carried out with an EG&G model 173 potentiostat. A three-electrode system was used consisting of a glassy carbon or platinum disk working electrode, a platinum wire counter electrode and a saturated calomel reference electrode (SCE). The SCE electrode was separated from the bulk of the solution by a fritted-glass bridge of low porosity that contained the solvent/supporting electrolyte mixture. Half-wave potentials were calculated as $E_{1/2} = (E_{pa} + E_{pc})/2$ and are referenced to SCE.

2.2. *Materials*

All reagents and solvents were of commercial reagent grade and used without purification. Dry dichloromethane was obtained according to published procedures [17]. Silica gel (100–200 mesh) was used for column chromatography. The tetra-*n*-butylammonium tetrafluoroborate was prepared according to reported methods [18].

2.3. *Synthesis of porphyrin dimer (1a, 1b)*

A solution of 200 mg of porphyrin **2a** or **2b** in 100 mL of dried dichloromethane was stirred at ice and salt bath temperature for 20 min. After addition of 89 mg of dicyclohexylcarbodiimide (DCC), the solution was stirred at 0°C for 12 h. After filtration through a glass frit under vacuum and concentration, the crude product was chromatographed on silica gel eluting with dichloromethane. The first fraction was collected and evaporated to dryness and chromatographed for a second time on the same column, then TLC was done.

3. Results and discussion

3.1. *Thermogravimetric analyses*

TGA-DTA analyses were done to determine mass loss of porphyrin **1a** [figure 1(b)] and **2a** [figure 1(a)]. A gradual weight loss at 150–400°C for **1a** (17.3% w/w loss) was assigned to loss of benzoic anhydride and at 150–300°C and 300–430°C for **2a** (6.8% w/w and 11.6% w/w loss) to loss of carboxyl and phenyl from porphyrin, respectively. A second rapid weight loss in the range 400–627°C for **1a** and 430–600°C for **2a** were attributed to the decomposition of the porphyrin. DTA showed two major weight losses at 327, 588°C for **1a** and at 347, 584°C for **2a**. In the simultaneous TGA-DTA analyses we observed no phase transition without mass loss.

3.2. *Surface photovoltage spectroscopy*

p-Type and *n*-type semiconductors depend on the sign of the bands associated with the SPV onset: $\delta V = V_s' - V_s^o$, where V_s' and V_s^o are the surface potential heights before and after illumination, respectively [19]. Band to band transitions occur when excitation energy is stronger than the forbidden bandwidth; electrons are excited to the conduction band, while holes are left in the valence band. Under the action of the built-in field, holes in the valence band move toward the bulk, while electrons in the conduction band diffuse

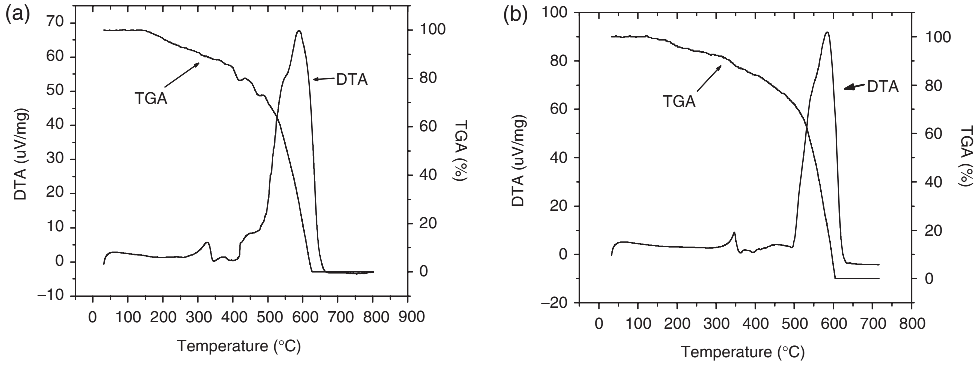

Figure 1. TGA-DTA thermograms showing the onset temperatures for weight loss of **1a** and **2a**.

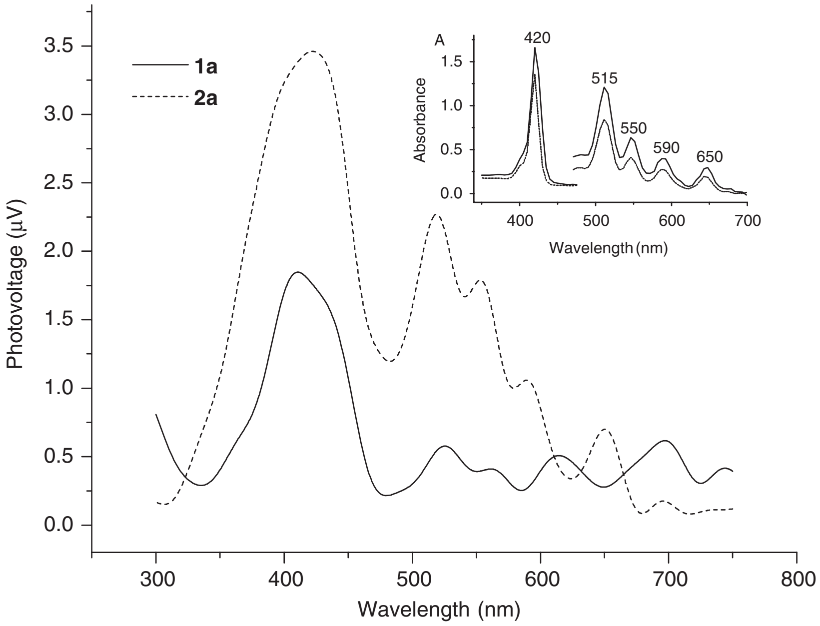

Figure 2. Surface photovoltage and UV–Vis (inset) spectra of **1a** and **2a** without an external field.

to the surface, resulting in a net positive charge in the space-charge region; band bending decreases and δVs is positive. These samples are all *p*-type semiconductors.

Porphyrins, as large π-conjugated systems, have obvious organic semiconducting characteristics and were found to be *p*-type semiconductors [20]. The bonding π orbital was analogous to the valence band, and the antibonding one to the conduction band. Photogenerated charge carriers in the π system were nonlocalized and their motion was free within the energy band of the π system. Photogenerated holes moved in the valence band, and photogenerated electrons in the conduction band. For this kind of system, the band to band transition was characterized as $\pi \rightarrow \pi^*$, exhibiting chiefly Soret and Q bands. Figure 2 shows the photovoltage response and UV–Vis spectrum (inset) of **1a** and **2a** in the region 300–700 nm; the Soret band manifested a strong positive photovoltage response.

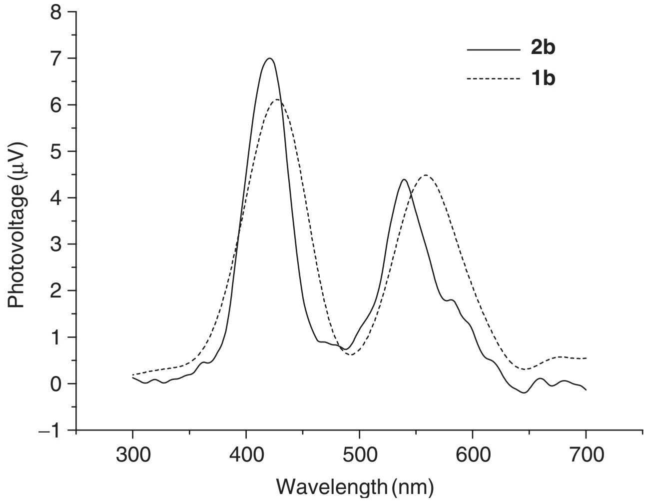

Figure 3. Surface photovoltage spectra of **1b** and **2b** without an external field.

The shapes of photovoltage action spectra were similar to the absorption spectra of the samples. The Soret band appears significantly broader than the absorption spectra due to the fact that SPS was the photoresponse of coacervation phase of the sample and absorption spectra show the light-absorbed process of a single molecule in solution. Similar results for zinc porphyrin dimer **1b** and zinc monomer **2b** are shown in figure 3. The SPV response of dimer **1a** is weaker than that of monomer **2a**. It is reasonable to deduce that the fluorescence intensity of **1a** is much stronger than that of monomer **2a** [16] and photogenerated electron-hole pairs of dimer **1a** are recombined quickly by means of fluorescence emission and cannot be effectively separated. As a result, dimer **1a** is unable to make a distinct SPV response. On the contrary, monomer **2a** is able to make a distinct SPV response.

Because the difference of fluorescence intensity for **1b** and **2b** is very small [16] and the photogenerated electron-hole pairs are separated more effectively than that of corresponding free base porphyrin, the SPV response intensities are similar and stronger.

The SPV response of **2a** with different external electric fields is given in figure 4. Comparing the spectral peaks, it is found that there is a simultaneous response with a change in the positive or negative electric field intensity. The SPV response is positive in a positive field but negative in a negative electric field. There is high symmetry in the changes of the response intensity with the strengthening of the two opposed electric fields, and the SPV response bands always appear at the same wavelength, no matter what external electric field is applied. Similar phenomenon for **1a** has been seen (not shown). A simultaneous response to the electric field indicates that all peaks can be assigned to $\pi \rightarrow \pi^*$ transitions. The response of the Q band is induced in a positive electric field. Being consistent with the Soret band, this is due to the fact that the external electric field reduces the recombination rate of photogenerated charges and prolongs the lifetime of the excited state.

The field-induced surface photovoltage spectroscopy (FISPS) of zinc monomer **2b** is shown in figure 5. Although the intensities of all peaks are different, their responses to the external electric field are the same as **1a**, positive in positive field but negative in a negative electric field. The dependence of photovoltage for **2b** on the applied voltage is

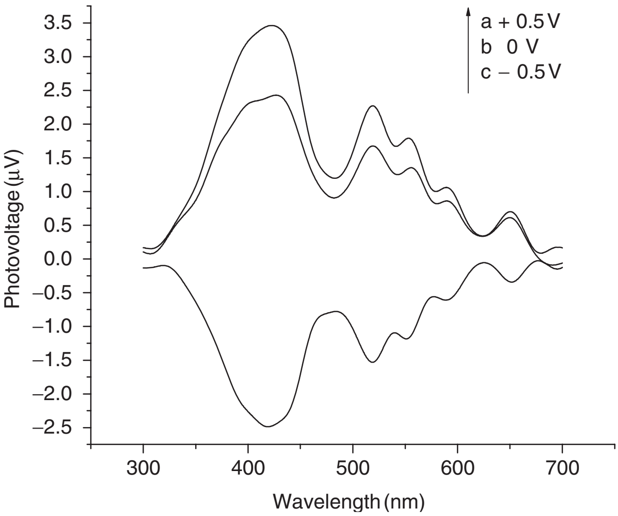

Figure 4. Surface photovoltage spectra of **2a** under positive and negative external fields.

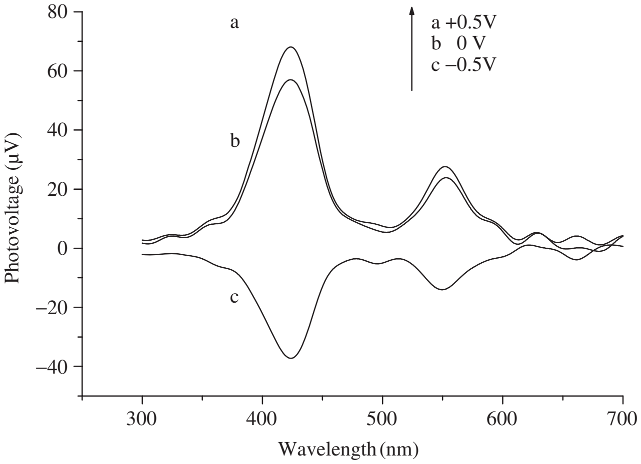

Figure 5. Surface photovoltage spectra of **2b** under positive and negative external fields.

almost symmetric for positive and negative fields. This interesting result is analogous to the electro-optical memory effect observed by Bard *et al.* [20].

In early research on fluorescence of porphyrin dimers, the results showed that fluorescence intensity of dimers (**1a** and **1b**) is stronger than those of related monomers [16b]. Comparing with the SPV spectra, the stronger the fluorescence intensity, the weaker the surface photovoltage intensity.

3.3. *Electrochemistry*

Electrochemistry of **1a** and the corresponding monomer **2a** were examined in DMF containing 0.1M TBAP. The cyclic voltammograms for these compounds are illustrated in figure 6 and the redox potentials are summarized in table 1. The monomer **2a**

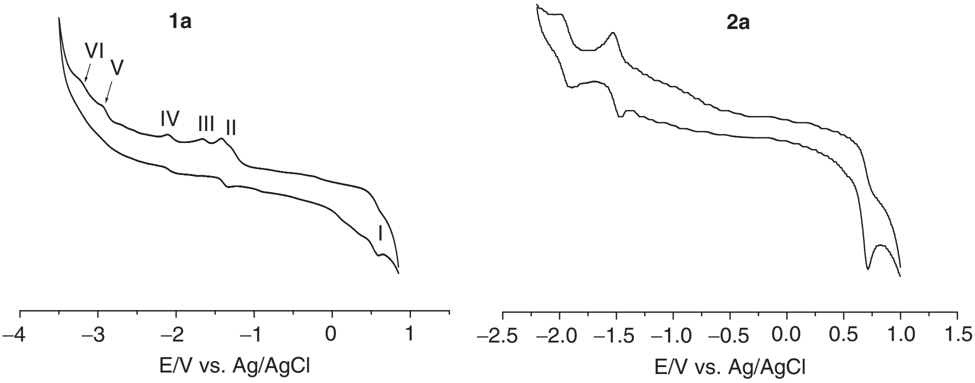

Figure 6. Cyclic voltammograms of **1a** and **2a** in DMF containing 0.1 M TBAP, scan rate = 60 mV s^{-1}.

Table 1. Summary of half-wave potentials ($E_{1/2}$/V) or peak potential (E_{pc}/V) in dry DMF containing 0.1 M TBAP.

	Oxidation		Reduction				
Compound	Dication	Cation	Anion	Dianion	Trianion	Tetraanion	Pentaanion
1a		0.62	−1.38	−1.63	−2.08	−2.92	−3.20
2a		0.71	−1.50	−1.94			
1b	0.57	0.37	−1.89	−2.31	−2.61	−3.15	
2b	0.68	0.47	−1.76	−2.18			

undergoes one irreversible oxidation (figure 6) at $E_{pc} = 0.71$ V; there are also two reductions at $E_{1/2} = -1.50$ V and $E_{1/2} = -1.94$ V at a scan rate of 0.06 V s^{-1}. The irreversible oxidation, assigned to a ring-based process, results in formation of the π-cation radical. The two reversible reductions, assigned to a stepwise gain of one electron by the porphyrin macrocycle, result in the formation of π-anion and π-dianion radicals [21–23].

Dimer **1a** shows six identifiable redox processes (I–VI), characteristic of a multi-electron redox species. The dimer undergoes only one irreversible oxidation in DMF with E_{pc} values located at 0.62 V assigned to the abstraction of one electron from any porphyrin macrocycle of dimer. The potential value is smaller than that of the corresponding monomer, consistent with a π–π interaction between the two porphyrin units [24], indicating dimer is easier oxidized. Electroreduction of dimer occurs in five steps, the first two of which are reversible and the result of a split reduction for formation of dianion with $E_{1/2}$ values located at −1.38 and −1.63 V. The first two reductions of **1a** can be assigned to a stepwise gain of one electron by each porphyrin. Because of the π–π interaction, both porphyrin macrocycles in **1a** are stepwise reduced at different potentials compared with the corresponding monomeric **2a** [22]. The monomer is reduced at −1.50 V, and when the wave is split, one process becomes easier and the other harder. This is shown in table 1 for **1a**. The third step is reversible but the fourth step irreversible, assigned to a stepwise addition of one electron to each porphyrin for formation of the tetraanion with $E_{1/2}$ values located at −2.08 and −2.92 V. Both reductions of dimer also occur at more negative potentials than those for reduction of **2a**, consistent with a π–π interaction between the two units in **1a** [24].

The potential separation between the first two reductions of dimer is 250 mV, a value much smaller than that between the third and fourth reductions where the potential separation is 840 mV. The last reduction is irreversible for formation of the pentaanion with $E_{1/2}$ values located at −3.20 V.

Displacement of two protons in the inner porphyrin core with a metal ion usually leads to a shift of the first ring-based reduction potential to a more negative value as a result of π-back donation of the filled d_π of the metal ion into the empty porphyrin π^* orbitals [23, 25]. Thus, as expected, introduction of zinc (i.e. the formation of **1b** and **2b**) resulted in shift of the ring processes to more negative values (compare the free base porphyrins and corresponding metal porphyrins, table 1). The cyclic voltammograms for **1b** and **2b** are illustrated in figure 7 and the redox potentials are summarized in table 1. The monomeric zinc porphyrin **2b** shows four identifiable redox processes (figure 7). Two reversible oxidation peaks at $E_{1/2} = 0.68$ V and $E_{1/2} = 0.47$ V are due to formation of the monocation and dication radicals of the zinc(II) porphyrin. Remarkably, the two oxidation processes of **2b** show large negative shifts ($\Delta E = 30$ and 240 mV, respectively), in comparison to the oxidation of **2a** at 0.71 V, due to introduction of zinc. Because of the introduction of zinc, two reversible reduction potentials at −1.50 V and −1.94 V for **2a** shift to −1.76 V and −2.18 V for **2b** which are assigned to a stepwise gain of one electron by the porphyrin. The same trend is seen in table 1 for the redox process of zinc dimer **1b** compared to that of the free base dimer **1a**.

Comparing zinc dimer **1b** and the corresponding zinc monomer **2b**, both show two reversible oxidations, however, the half-wave potentials of 0.68 and 0.47 V for **2b** shift to 0.57 V ($\Delta E = 110$ mV) and 0.37 V ($\Delta E = 100$ mV) for **1b**, indicating that **1b** is easier to oxidize than **2b** due to the internal interaction between the two π-systems of the dyad [24]. Electroreduction of zinc dimer **1b** occurs in four steps, the first two of which are reversible and the result of a split reduction for formation of dianion radical with $E_{1/2}$ values located at −1.89 and −2.31 V. The latter two reductions are irreversible and the result of a split reduction for formation of quadrivalent anion radical with $E_{pc} = -2.61$ and $E_{pc} = -3.15$ V. The potential separation between the first two reductions of **1b** is 420 mV and 540 mV between the latter two irreversible reductions. The larger potential separation between the first two reductions of **1b** compared to **1a** (table 1) can be attributed to a larger π–π interaction between the two porphyrin macrocycles after introduction of zinc.

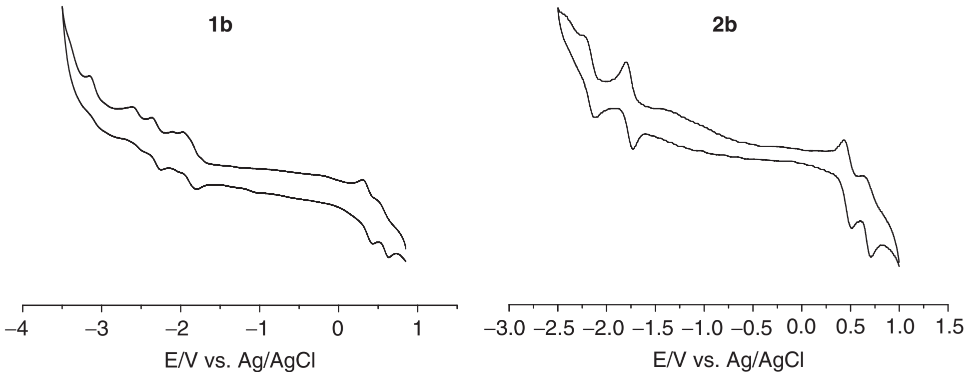

Figure 7. Cyclic voltammograms of **1b** and **2b** in DMF containing 0.1 M TBAP, scan rate = 60 mV s^{-1}.

The larger the internal interaction between the two π systems of the dyad, the harder the reduction is and the easier the oxidation is [26], leading to easier oxidation and more difficult reduction for zinc dimer than the free base dimer.

3.4. *EPR spectra*

Further indications of the nature of the dimers are provided by electron paramagnetic resonance (EPR) spectroscopy (in solid state). The EPR spectra of **1a** and **2a** at 77 K after illumination by visible light are shown in figure 8. The free base porphyrins have no EPR signal before illumination. The signal intensity is increased with the time after illumination. The EPR spectrum of monomer **2a** shows a nine-line superhyperfine splitting due to the interaction between delocalized π electron and N magnetic nuclei. The signal of dimer **1a** exhibits a thirteen-line superhyperfine splitting due to the four nitrogens and four quasi-equivalent nitrogen atoms of dimer. The g value (2.0010) of **1a** radical complex that is smaller than the value of the monomer radical complex (2.0018) results from interaction between the two porphyrin macrocycles of **1a**. EPR hyperfine broadening of **1a** compared to monomer **2a** is primarily due to π–π interaction. Superposition of the field of the neighboring molecules on the external magnetic field leads to a spread of resonance frequencies within each quantum level of the paramagnetic system [27]. This results in spin–spin dipolar broadening of the spectral lines.

Figure 9 shows the EPR spectra of zinc dimer and the corresponding monomer at room temperature. The central zinc ions has no unpaired electron and so the

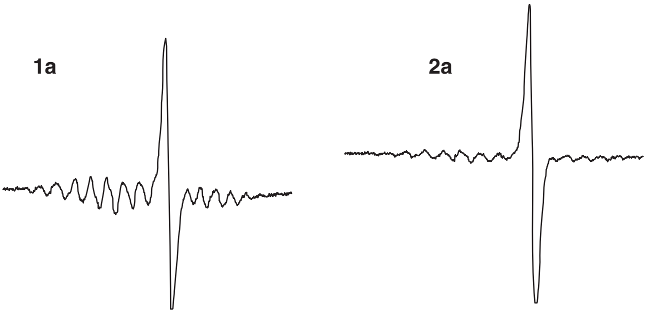

Figure 8. EPR spectra of **1a** and **2a** at 110 K.

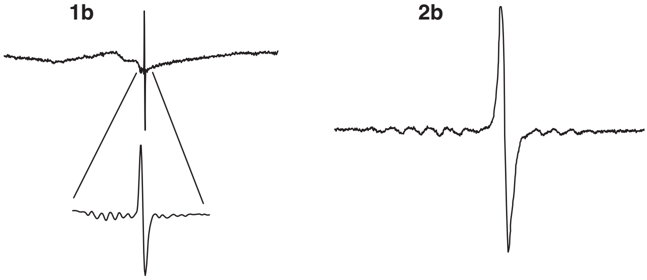

Figure 9. EPR spectra of **1b** and **2b** at room temperature.

appearance of the EPR signals of **2b** is the same as that for the metal-free porphyrins, and that of **1b** in which coordination with the two zinc ions could barely be seen.

4. Conclusion

A comparative study of the free base dimer and zinc dimer and their related monomeric porphyrins shows that electronic interaction appears in the dimer system. Through thermogravimetric analyses, porphyrin dimer was stronger than porphyrin monomer in stabilization of configuration. The SPV and FISPS indicate that they are *p*-type semiconductors and the stronger the fluorescence intensity, the weaker the surface photovoltage intensity. The electrochemistry and EPR of the porphyrins show clearly that a π–π interaction exists between the two macrocycles of dimer as compared to those of related monomers.

Acknowledgements

We gratefully acknowledge the support of this research by the National Science Foundation of China (20071014, 20273027, 20701023, 30770568) and National 863 Plans Projects of China (2006AA04z349).

References

[1] (a) M.R. Wasielewski. *Chem. Rev.*, **92**, 435 (1992); (b) R.W. Wagner, J.S. Lindsey. *J. Am. Chem. Soc.*, **116**, 9759 (1994); (c) J.S. Hsiao, B.P. Krueger, R.W. Wagner, T.E. Johnson, J.K. Delaney, D.C. Mauzerall, G.R. Fleming, J.S. Lindsey, D.F. Bocian, R.J. Donohoe. *J. Am. Chem. Soc.*, **118**, 11181 (1996); (d) S.I. Yang, J. Seth, T. Balasubramanian, D. Kim, J.S. Lindsey, D. Holten, D.F. Bocian. *J. Am. Chem. Soc.*, **121**, 4008 (1999).

[2] J.Y. Zheng, K. Konishi, T. Aida. *Tetrahedron*, **53**, 9115 (1997).

[3] (a) J.P. Collman. *Inorg. Chem.*, **36**, 5145 (1997); (b) M.L. Merlau, M. del Pilar Mejia, S.T. Nguyen, J.T. Hupp. *Angew. Chem. Int. Ed.*, **40**, 4239 (2001).

[4] D. Gust. *Nature*, **386**, 21 (1997).

[5] (a) H. Segawa, D.Y. Machida, J. Nakazaki, K. Hirakawa, F. Wu. *Chem. Commun.*, **24**, 3032 (2002); (b) H. Segawa, Y. Senshu, J. Nakazaki, K. Susumu. *J. Am. Chem. Soc.*, **126**, 1354 (2004).

[6] V. Balzani, F. Scandola. *Supramolecular Photochemistry*, Ellis Horwood, Chischester, UK (1991).

[7] V. Balzani, F. Scandola. *Compr. Supramol. Chem.*, **10**, 687 (1996).

[8] Molecular Electronics (J. Jortner, M. Ratner), Blackwell Science, London (1997).

[9] (a) C. Joachim, J.K. Gimzewski, A. Aviram. *Nature*, **408**, 541 (2000); (b) Y. Shirota. *J. Mater. Chem.*, **10**, 1 (2000).

[10] (a) G.C. Allen, N.S. Hush. *Prog. Inorg. Chem.*, **8**, 357 (1967); (b) C. Joachim. *Chem. Phys.*, **116**, 339 (1987); (c) S. Larsson. *Chem. Phys. Lett.*, **90**, 136 (1982).

[11] (a) Y. Deng, C.K. Chang, D.G. Nocera. *Angew. Chem., Int. Ed.*, **39**, 1066 (2000); (b) I.M. Blake, L.H. Rees, T.D.W. Claridge, H. Anderson. *Angew. Chem., Int. Ed.*, **39**, 1818 (2000); (c) R.G. Khoury, L. Jaquinod, K.M. Smith. *Chem. Commun.*, **11**, 1057 (1997); (d) K. Susumu, T. Shimidzu, K. Tanaka, H. Segawa. *Tetrahedron Lett.*, **37**, 8399 (1996); (e) L. Jaquinod, M.O. Senge, R.K. Pandey, T.P. Forsyth, K.M. Smith. *Angew. Chem. Int. Ed.*, **35**, 1840 (1996); (f) H. Segawa, Y. Senshu, J. Nakazaki, K. Susumu. *J. Am. Chem. Soc.*, **126**, 1354 (2004); (g) T. Ishizuka, A. Osuka, H. Furuta. *Angew. Chem. Int. Ed.*, **43**, 5077 (2004); (h) P.J. Chmielewski. *Angew. Chem. Int. Ed.*, **43**, 5655 (2004).

[12] (a) Y. Shimazaki, H. Takase, T. Chishiro, F. Tani, Y. Naruta. *Chem. Lett.*, **30**, 538 (2001); (b) J.T. Fletcher, M.J. Therien. *J. Am. Chem. Soc.*, **122**, 12393 (2000); (c) A. Osuka, G. Noya,

S. Taniguchi, T. Okada, Y. Nishimura, I. Yamazaki, N. Mataga. *Chem. Eur. J.*, **6**, 33 (2000); (d) J. Li, J.S. Lindsey. *J. Org. Chem.*, **64**, 9101 (1999); (e) R. Beavington, P.L. Burn. *J. Chem. Soc., Perkin Trans. 1*, **999**, 583 (1999); (f) G. Hungerford, M. Van der Auweraer, J.C. Chamborn, V. Heitz, J.P. Sauvage, J.L. Pierre, D. Zurita. *Chem. Eur. J.*, **5**, 2089 (1999); (g) D.A. Shultz, H. Lee, R.K. Kumar, K.P. Gwaltney. *J. Org. Chem.*, **64**, 9124 (1999); (h) A.K. Burrell, D. Officer. *Synlett*, **1998**, 1297 (1998).

[13] J.Y. Zheng, K. Tashiro, Y. Hirabayashi, K. Kinbara, K. Saigo, T. Aida, S. Sakamoto, K. Yamaguchi. *Angew. Chem., Int. Ed.*, **40**, 1858 (2001).

[14] (a) I.M. Dixon, J.P. Collin, J.P. Sauvage, F. Barigelletti, L. Flamigni. *Angew. Chem. Int. Ed.*, **39**, 1292 (2000); (b) E. Iengo, B. Milani, E. Zangrando, S. Geremia, E. Alessio. *Angew. Chem. Int. Ed.*, **39**, 1096 (2000).

[15] C. Ikeda, N. Nagahara, E. Motegi, N. Yoshioka, H. Inoue. *Chem. Commun.*, **17**, 1759 (1999).

[16] (a) H.B. Fa, L. Zhao, X.Q. Wang. *Chem. J. Chinese U.*, **27**, 17 (2006); (b) H.B. Fa, W. Yin, W.Q. Zheng, D. Li, N. Shan, X.Q. Wang. *Chem. Res. Chinese U.*, **22**, 684 (2006).

[17] W.D. Huang, C.Q. Chen. *Synthesis of Peptide [M]*, Vol. 9, Science Press, Beijing (1985).

[18] H.O. House, E. Feng, N.P. Peet. *J. Org. Chem.*, **36**, 2371 (1971).

[19] D.J. Wang, W. Liu, L.Z. Xiao, T.J. Li. *Chem. Bull.*, **10**, 32 (1989).

[20] B.A. Gregg, M.A. Fox, A.J. Bard. *J. Phys. Chem.*, **94**, 1586 (1990).

[21] (a) C. Inisan, J.Y. Saillard, R. Guilard, A. Tabard, Y.L. Mest. *New J. Chem.*, **22**, 8231 (1998); (b) H. Sun, J.C. Biffinger, S.G. Dimagno. *Dalton Trans.*, **19**, 3148 (2005).

[22] J.P. Hill, A.S.D. Sandanayaka, A.L. McCarty, P.A. Karr, M.E. Zandler, R. Charvet, K. Ariga, Y. Araki, O. Ito, F.D. Souza. *Eur. J. Org. Chem.*, **2**, 595 (2006).

[23] A.B.P. Lever, E.R. Milaeva, G. Speier. In *Phthalocyanines: Properties and Applications*, A.B.P. Lever, C.C. Leznoff (Eds), Vol. 3 Chap.1, pp. 1–69, VCH Publishers, New York (1993).

[24] (a) R. Guilard, F. Jerome, J.M. Barbe, C.P. Gros, Z.P. Ou, J. Shao, J. Fischer, R. Weiss, K.M. Kadish. *Inorg. Chem.*, **40**, 4856 (2001); (b) R. Guilard, C.P. Gros, J.M. Barbe, E. Espinosa, F. Jerome, A. Tabard. *Inorg. Chem.*, **43**, 7441 (2004).

[25] A.R. Özkaya, A.G. Gürek, A. Gül, Ö. Bekaroğu. *Polyhedron*, **16**, 1877 (1997).

[26] K.M. Kadish, J. Shao, Z. Ou, L. Frémond, R. Zhan, F. Burdet, J.M. Barbe, C.P. Gros, R. Guilard. *Inorg. Chem.*, **44**, 6744 (2005).

[27] A. MacCragh, C.B. Storm, W.S. Koski. *J. Am. Chem. Soc.*, **87**, 1470 (1965).